

THE CLARK LAKE TEEPEE-TEE TELESCOPE

W. C. ERICKSON, M. J. MAHONEY, AND K. ERB
Clark Lake Radio Observatory, University of Maryland
Received 1982 February 22; accepted 1982 April 20

ABSTRACT

A new, fully steerable, decametric array for radio astronomy has been built at the Clark Lake Radio Observatory near Borrego Springs, California. This array is a "T" of 720 conical spiral antennas (teepee-shaped antennas), 3.0 km by 1.8 km. It is capable of operating between 15 and 125 MHz but has best sensitivity in the 25 to 75 MHz range. Both its operating frequency and beam position are adjustable in ~ 1 ms.

A 1024 channel digital correlator has been built and attached to the array. This permits the simultaneous measurement of the complex visibility functions on 512 interferometer baselines between various portions of the array. After Fourier transformation these visibility data yield a 32×32 resolution element picture of the area of sky under observation, with frequency-dependent angular resolution ranging from $20''$ to $2.7''$ and a sensitivity of 1 Jy per beam. The system is described, and some initial observations are presented.

Subject headings: instruments — interferometry

1. INTRODUCTION

The design of the Clark Lake Teepee-Tee (TPT) has been described in a previous paper (Erickson and Fisher 1974, hereafter Paper I). The rationale for building the system was that a flexible telescope, capable of multi-frequency operation and of being steered in two coordinates, was required in order to carry out detailed studies of radio sources, including the Sun, at meter-decameter wavelengths. The lack of such a system has kept long wavelength radio astronomy at a primitive level compared with astronomy at shorter wavelengths.

A novel antenna element design was developed for this project. It is a log-spiral element utilizing eight wires wound around a support system that consists of eight parallel filament, dacron ropes. The ropes are protected by polyethylene jackets. Each element is circularly polarized with a diode switch at its apex which rotates its excitation and thus adjusts its phase. The N-S arm of the array is shown in Figure 1, and the layout of the system is illustrated in Figure 2.

Steering of the array is accomplished by putting a linear phase gradient across groups of 15 contiguous elements, called banks. There are 32 banks in the 3000 m E-W arm of the "T" and 16 banks in the 1800 m N-S arm. The output of each bank is brought separately to the central observatory building. Paper I contains a detailed discussion of the design and testing of the antennas. The specifications of the system are given in Table 1.

The main array contains 720 left circularly polarized elements. A secondary, right circularly polarized array of 48 elements has also been constructed by placing one

right circular element adjacent to the main array, near the center of each bank. This forms a grating array whose length is equal to that of the main array, but whose collecting area is $1/15$ as large. This grating array is useful for solar studies.

A separate receiver channel is attached to the output of each of the 48 banks. Each channel employs an up conversion from the frequency being observed to 170 MHz. This conversion places all image frequencies well above the frequency range of observation. After some amplification, the signals are converted to 10 MHz where the principal amplification occurs. Four IF bandwidths, ranging from 3 to 0.15 MHz, are selectable. A diagram of these channels is shown in Figure 3.

In Paper I we described a receiving system in which the signals from the various banks would be combined using beam forming networks to produce 49 simultaneous beams. This design was discarded in lieu of an aperture synthesis type system in which each E-W bank output is digitally cross-correlated with each N-S output. This requires 512 complex (sine and cosine) correlations, i.e., a total of 1024 correlators.

The 10 MHz output of each receiver channel is sampled at a frequency of 12 MHz, digitally delayed, and then cross-correlated. The correlator outputs from the 512 simultaneous interferometers are preintegrated for periods from 10 ms to 10 s—periods short enough that the phase rotation for a source moving at a sidereal rate is negligible on any of the interferometer baselines—and after each preintegration period, the digital data are written on magnetic tape. Later, an off-line processor is used to remove the phase rotation and to integrate the

¹Originally published in the ApJS, Vol. 50, p.403, 1982 - Reproduced with permission

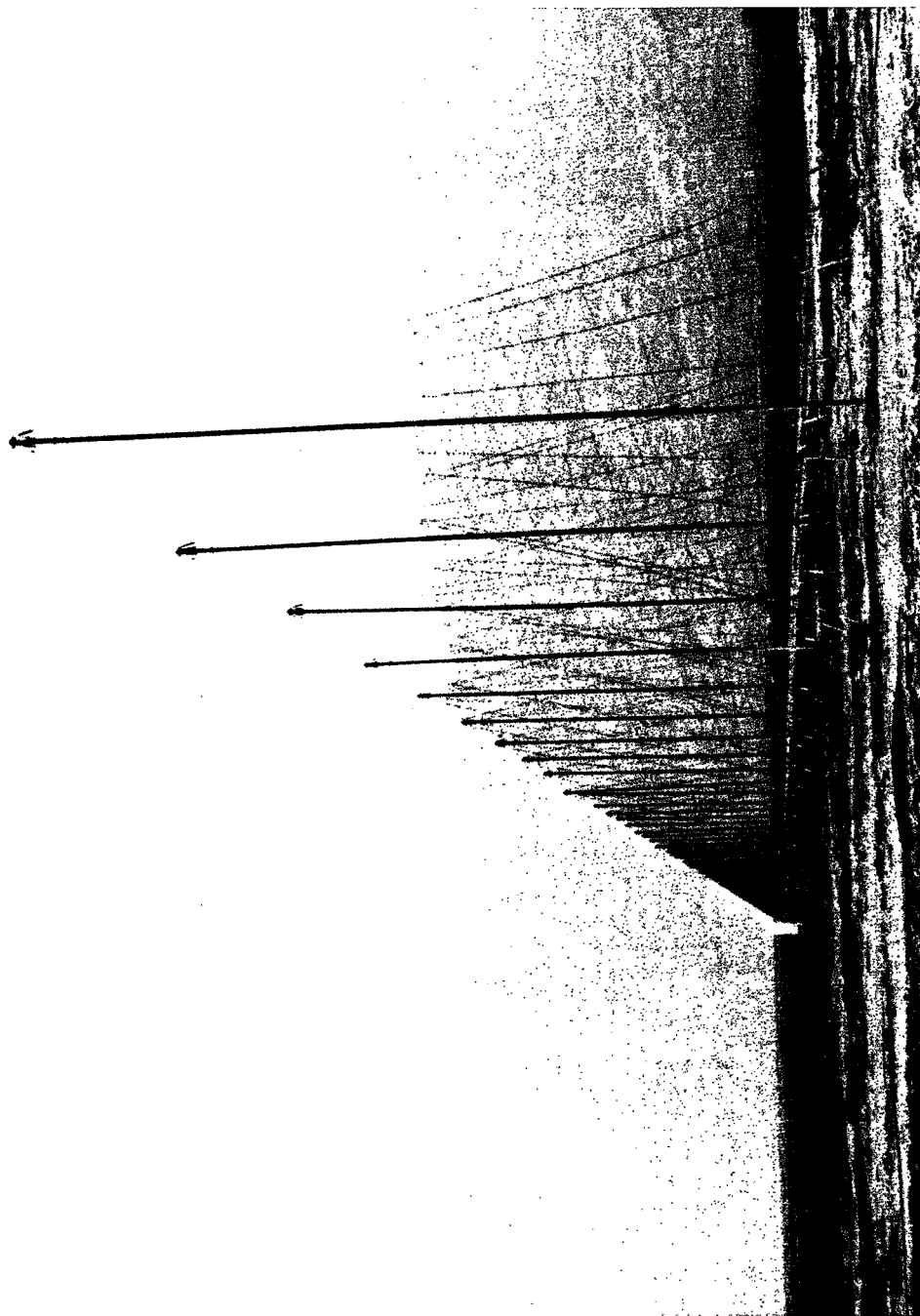


FIG. 1.—Clark Lake TPT telescope. This is a view of 240 elements in the S arm.

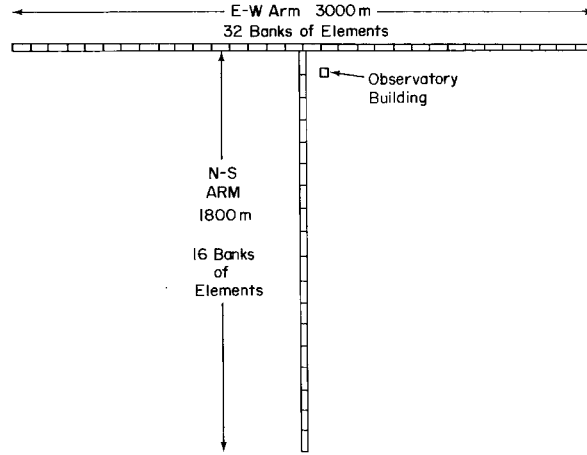


FIG. 2.—Layout of the T. The signal from each bank of elements is amplified and transmitted to the observatory by separate, equal length coaxial cables.

TABLE 1
TPT SPECIFICATIONS

Parameter	Value
Frequency range	15–125MHz
Instantaneous bandwidth	0.15–3 MHz
Total collecting area.....	$250\lambda^2$
Resolution	
20 MHz	17'
110 MHz	3'
Steering and frequency changing time ..	$\ll 1$ ms
Sky coverage	$< 45^\circ$ zenith distance
Sensitivity (and confusion limit)	~ 1 Jy at all frequencies
Polarization	left circular

signals for periods of up to 5 minutes. A Fourier transform then produces a map of the area of sky under observation. These maps may be averaged to effectively integrate the signals for periods of hours. Since the antenna was described in Paper I, this paper will describe the digital hardware and software systems and will present some initial results. A detailed description of the electronics system is to be found in von Arx, Calffisch, and Erickson (1978).

II. DIGITAL HARDWARE

a) General Considerations

The digital hardware must provide the 512 correlation coefficients by correlating each of the 32 banks in the E-W arm with each of the 16 banks in the N-S arm.

Each N-S arm signal is split into two orthogonal components, and each of these components is individually correlated with the other signal, thus providing the real and imaginary parts of the complex correlation coefficient. Generation of the orthogonal phases digitally would have been more complicated, so the 16 signals from the N-S arm are divided by analog quadrature hybrids. The quadrature hybrids are accurate to $\pm 2^\circ$ and are placed ahead of the samplers. The layout of the digital system is shown in Figure 4.

For observations away from the zenith at relatively large bandwidths, it is necessary to delay the signals appropriately before correlation in order to preserve coherence. Figure 4 shows the general layout of the analog to digital converters, delay lines, and correlators.

The complexity of the hardware required for this system suggested the use of digital correlators. Digital correlation allows very coarse amplitude sampling with relatively little loss in sensitivity. This loss of sensitivity is determined by the number of quantization levels and the oversampling factor,

$$K = \frac{\text{actual sampling rate}}{\text{Nyquist sampling rate}}.$$

With increasing K , the sensitivity loss becomes smaller and asymptotically approaches a theoretical minimum (Klinger 1972). We use three-level quantization and a minimum oversampling factor of 4. The resultant loss of sensitivity is 13% relative to analog correlation when a 3 MHz bandwidth is employed; at narrower bandwidths the loss is smaller.

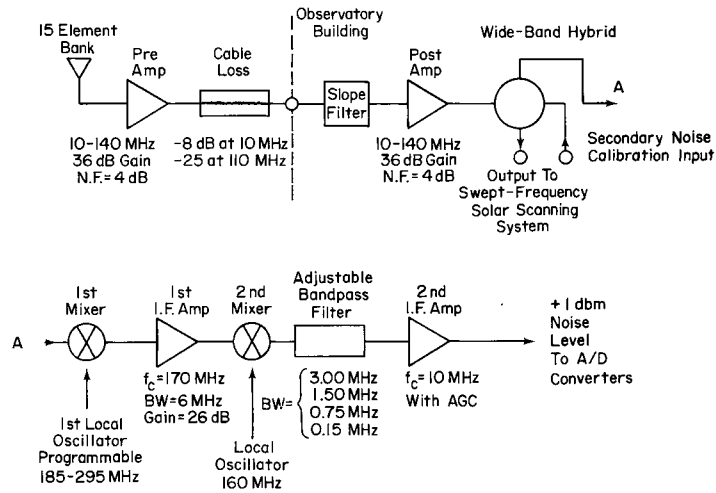
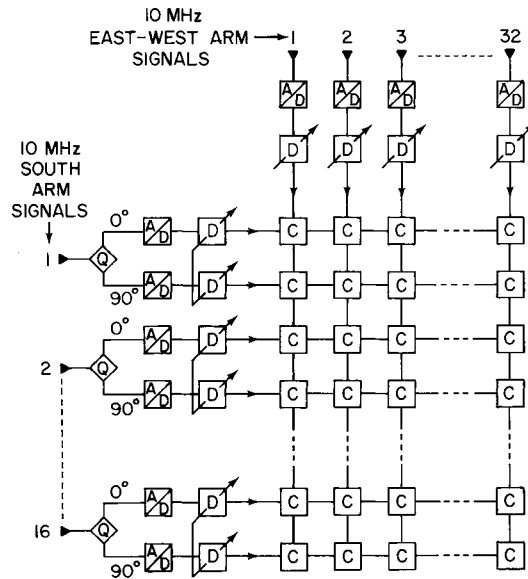


FIG. 3.—Schematic diagram of one of the 48 analog receiver channels

FIG. 4.—Layout of the digital hardware. The legend for the various components is as follows: Q = analog quadrature hybrid power splitter; A/D = three-level analog to digital converter, 12 MHz clock frequency; D = digital delay lines, adjustable from 83.3 ns to 10.6 μ s in steps of 83.3 ns; C = digital correlator and accumulator.

The use of digital delays implies that the time delay can only be changed in discrete steps. For the 12 MHz sampling rate, this increment is 83.3 ns. This restriction, however, is tolerable since the maximum delay error causes a maximum sensitivity loss of $\sim 2.5\%$ at the largest bandwidth of 3 MHz.

The three-level sampling (assuming fixed decision thresholds) requires a fairly constant level of the analog input signal. This is provided by sensitive and fast automatic gain control (AGC) in the 10 MHz amplifiers. The time constant of the AGC loops is 1 ms. The AGC, unfortunately, causes a nonlinear relationship between the measured correlation coefficient, C , and the true correlated power, S :

$$C \propto \frac{S}{S + \sqrt{N_1} \sqrt{N_2}},$$

where N_1 and N_2 are the uncorrelated noise levels at the inputs of the two channels. This relation is based on the assumptions that both analog output levels are equal and constant. When the correlation is low, the factor between S and C can be determined by periodic calibration. When strong sources, such as solar bursts, are observed, a correction will have to be applied to the measured correlations. This correction can be calculated by sensing the AGC levels or by very frequent channel gain calibration.

In spite of careful shielding between RF cables, amplifiers, IF cables and A/D converters, there is inevitably a certain amount of crosstalk between individual channels which causes low level spurious correlations. We employ Walsh function phase switching to reduce this effect. Assuming that most of the crosstalk occurs in the IF amplifier or in the A/D converters (due to the

physical proximity and common power supplies), this portion of the signal path is periodically inverted using orthogonal binary sequences which control a phase switch in the second local oscillator line. Correlated signals mutually induced by crosstalk do not affect the correlator output if the two binary sequences are orthogonal and have an orthogonality interval equal to or an integer fraction of the integration interval.

When the system is used in the basic mode, where only E-W and N-S antenna outputs are cross-correlated, one row of inputs (E-W) can be left unswitched, and the other row of inputs (N-S) is periodically inverted. However, appropriate sets of Walsh functions are provided for correlating E-W or N-S outputs with themselves. Such correlations are necessary if phase closure techniques are to be employed.

Some very low level correlated signals (20 to 40 db below the noise level) have been found to be induced into the transmission line systems outside the observatory building. The cause of most of these spurious signals is, as yet, unknown. However, their effects have been eliminated by the introduction of a second phase inversion sequence. The phase of the correlated antenna signal is inverted in alternate samples by rotation of the diode-controlled antenna elements in one arm of the array. This phase modulation of the desired signal is subsequently demodulated in the data processing program.

b) Description of the 1024 Channel Hardware

Figure 5 is a block diagram of an A/D converter. The basic elements are three Am687 ECL comparators with latched outputs, producing a two-bit digital output according to Table 2. A two-level mode is provided for rapidly varying signals (such as solar bursts) where the

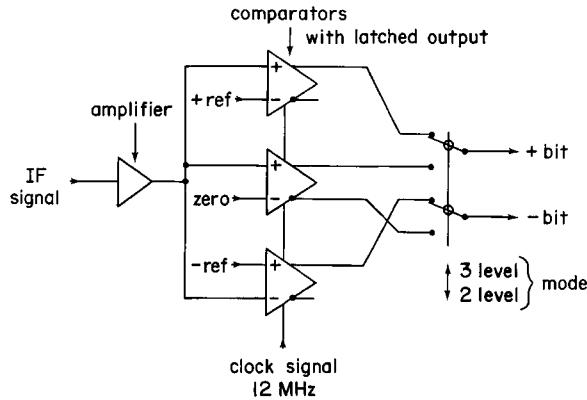


FIG. 5.—Two-level or three-level analog to digital converter

TABLE 2
QUANTIZATION LEVELS

Signal Amplitude	Symbolic Amplitude	+ bit	- bit
Three-Level Quantization			
Signal $> +U_{ref}$	+1	1	0
$-U_{ref} < \text{signal} < +U_{ref}$...	0	0	0
Signal $< -U_{ref}$	-1	0	1
Two-Level Quantization			
Signal > 0	+1	1	0
Signal < 0	-1	0	1

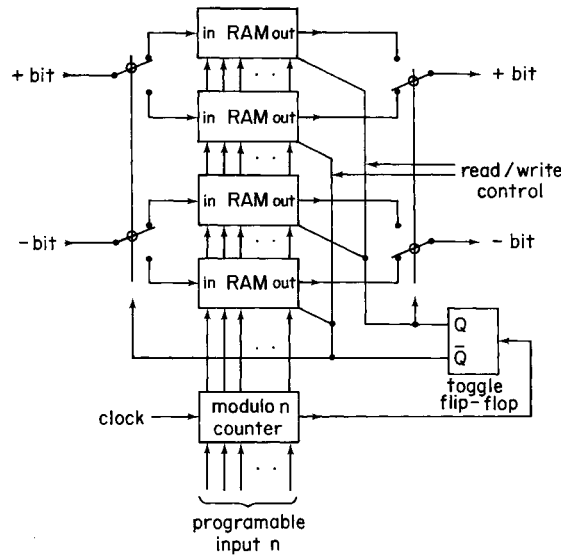


FIG. 6.—Programmable delay line

AGC may be too slow to maintain the constant signal level that is required for three-level quantization.

The programmable delay lines, illustrated in Figure 6, are based on a pair of random access memories (RAM), addressed by a modulo n counter. Input data are written into one memory, while output data are being read from the other memory. After each cycle of the modulo n counter, the two memories are swapped, thus providing a delay of $n + 1$ clock periods. The length of the cycle, n , is programmable from 0 to 127.

Thanks to the availability of the custom-made integrated circuits developed for the NRAO Very Large Array (VLA1 and VLA2), the amount of hardware

required for the 32×32 correlator matrix could be kept within reasonable limits. Figure 7 shows the basic concept of an individual correlator. In each clock period the multiplication logic adds a 0, 1, or 2 into a 14-bit ripple counter according to the multiplication scheme in Table 3. To avoid overflow, the counter is reset every 2^{13} clock periods after transferring the sum into a 12-bit shift register. Sufficient precision can be attained through the use of only the 10 most significant bits of the original 14 bits from the ripple counter. The shift registers of 16 correlators are cascaded and serially transferred into a microprocessor, which accumulates the sum in 16-bit registers. The correlators produce a constant offset be-

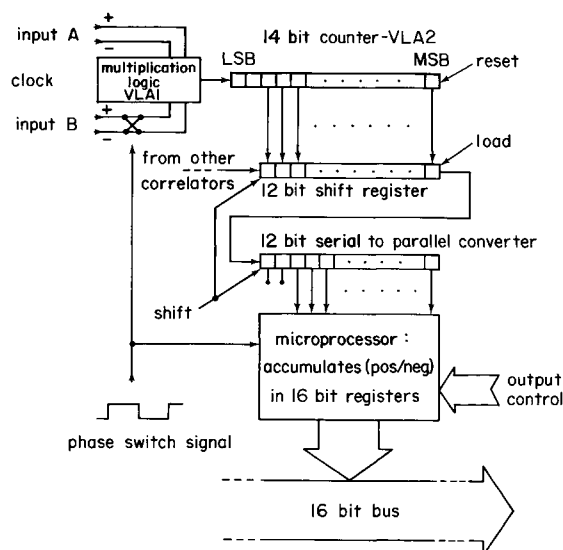


FIG. 7.—Schematic diagram of a correlator

TABLE 3
MULTIPLICATION SCHEME

INPUT B	INPUT A		
	+1	0	-1
+1	add 2	add 1	add 0
0	add 1	add 1	add 1
-1	add 0	add 1	add 2

cause zero correlation adds a 1 to the ripple counter; this effect is eliminated by periodically inverting one correlator input while simultaneously inverting the sign of accumulation in the microprocessor. The phase switch signal, which controls this inversion, has a period equal to the shortest integration interval. Zero correlation thus produces a zero output.

One microprocessor (R6505A) serves 16 individual correlators and, because of a double set of accumulation registers and time sharing, is able to simultaneously accumulate input data and transfer output data to a minicomputer through a common 16-bit data bus. For high speed operation, a special mode can be selected that causes the microprocessor to reduce the word length by logarithmic compression, allowing the simultaneous transfer of two numbers and operation with 10 ms time resolution.

In addition to the cross-correlators the system also contains 64 self-correlators, one for each digital input signal. Although the dynamic range of the self-correlation is very small (due to the AGC), this provides information for correction of AGC and sampler threshold errors. As yet, these corrections have not been implemented in the data reduction software.

c) Computer System

The following description refers to the schematic layout of the computer system shown in Figure 8. It is a dual processor system designed around two Perkin-Elmer processors: a 7/16 processor which controls the on-line functions of telescope control and data acquisition, and a 7/32 processor which performs off-line multiuser functions of program development and data reduction.

For high speed data transfers both processors use selector channels (selches) for direct memory access. In particular, the 7/16 uses one selch to input data from the correlator system (CXIN), and another to output data to magnetic tape (M1, M2). Without these selches the 7/16 would not be able to handle the 100 kB data rates required for high time resolution operation. The 7/32 uses selches to access high speed devices such as disk drives (D1, D2) and magnetic tape transports (M1, M2, M3, M4).

Selch programming and other low speed input and output (I/O) occurs over the multiplexor bus. Both

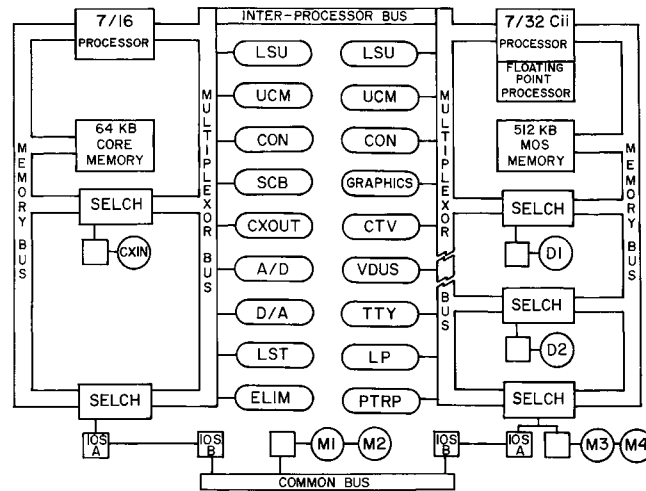


FIG. 8.—Computer hardware

processors use this bus to access a system console (CON), clock (UCM), and loader storage unit (LSU), which is used to boot the operating system. In addition to these functions, the 7/16 uses the multiplexor bus for telescope control (SCB), correlator programming (CXOUT), reading the sidereal clock (LST), and other related activities. On the 7/32 the additional functions of the multiplexor bus include access to the various interactive terminals (GRAPHICS, VDUs, TTY), a color television display (CTV), a printer/plotter (LP), and a paper tape reader and punch (PTRP).

It will be noted in Figure 8 that the processors are connected by two methods: an interprocessor bus (IPB) and a common bus. Although both these busses appear the same to both processors, they are under the strict control of the 7/16 so as to protect its on-line operation. The interprocessor bus is used by an observer to communicate with a management task running in the 7/32. Thus, it can be used to request stored information (such as observing programs), to manipulate files, or to control tasks (such as a task to transform transmitted visibility data). The common bus, on the other hand, is used simply to share peripherals between the two processors. It does this by means of I/O bus switches (IOS) on each processor.

III. TELESCOPE CONTROL AND DATA ACQUISITION SOFTWARE

A queue-oriented real time operating system called BORIS was developed to control the TPT and acquire the correlator data. Normally BORIS is down loaded

from the 7/32 over the interprocessor bus using one of several bootstrap programs. If, however, the IPB is inoperative, all its essential functions can be performed from magnetic tape, thus insuring the integrity of the system.

The basic concept used in developing BORIS was the I/O queue. That is, I/O buffers are taken as needed from a buffer pool, put on an I/O queue where they are processed, and then returned to the original buffer pool. With this approach, only two very simple subroutines are required to manage the system buffers: one to get buffers from a pool or a queue, and one to return them. In addition, the availability of buffers can be used to regulate various procedures, and buffers can be linked together to speed up data transfers.

All device handlers used in BORIS are fully interrupt driven, are noninterruptable, and run at the same priority level. However, since correlator input and magnetic tape output occur over the memory bus and are initiated by only a single interrupt, the longest delay in the data acquisition process is determined by the longest interrupt service routine not involved in data acquisition. Since all these routines execute much faster than the shortest integration time of 10 ms, there is no conflict.

Overall control within BORIS is maintained by a monitor program. This program checks for I/O queue activity and enters various routines to clear the queues. This includes routines to process commands, update the system status, calculate telescope steering data, manage the interprocessor bus, and so forth. In the absence of I/O queue activity, the monitor idles the processor so that memory bus data transfers can run at full memory

access speed. BORIS also includes a resident debugger program for trouble shooting, and a comprehensive correlator test program.

At the present time telescope steering information is calculated in the 7/32 and placed in a disk file for subsequent transferral to the 7/16 via the interprocessor bus. These steers provide settings for the digital delays, the phase steering, the first local oscillator frequency synthesizer, and the like. Using a system status monitor, the observer can interactively reconfigure the correlator operating characteristics and observation program. Provision is currently made for the time-shared observation of as many as 16 sources with separate time slices. This is possible because the telescope can be steered in a small fraction of the shortest integration period. Because hardware buffers are used to save upcoming correlator or steer information, only a single I/O command is required to reprogram the entire system at the end of an integration cycle. Finally, it should be noted that all observer dialogue, steer information, and error conditions are logged on the data tape along with the correlator outputs.

With a little more development, involving chiefly the implementation of fixed point trigonometric routines, the entire control of the telescope will be possible in real time using the 7/16 system console. The present mode of steering will be maintained, at least in part, to allow batch-type observations which minimize the amount of observer interaction required. In the batch mode, the system runs quite automatically.

IV. DATA REDUCTION SOFTWARE

a) Programs

Four FORTRAN programs are used for off-line data reduction in the 7/32 processor:

1. REDCOR reads the telescope data tape, calculates fringe rates for the 512 interferometer pairs, stops the fringes, and integrates the data for a period of a few seconds to a few minutes. It next displays the amplitudes and phases of the visibility functions on the color TV, Fourier transforms the visibility data, and outputs a map of the area of sky that was observed. The independent coordinates used in plotting the REDCOR output maps are the direction cosines with respect to the E-W and N-S arrays.

2. SYSCAL uses REDCOR output from observation of a point source calibrator to generate a file of observed phase shifts and gains for each of the 48 analog channels. These calibrated phases and gains are used by REDCOR in all subsequent processing.

3. SKYMAP selects REDCOR output maps that are free from terrestrial interference and strong source side-lobe responses. It then projects the selected maps onto equatorial coordinates and averages them. Data can thus be averaged for periods of several hours duration. SKYMAP also uses the beam pattern obtained in the

most recent calibration observation at a given observing frequency to estimate the beam at the time of observation. It projects these beam patterns onto equatorial coordinates to obtain an average map of the beam pattern that corresponds with the average data map. After completion of the observation, SKYMAP uses the CLEAN algorithm (Högbom 1974) to correct the data map for the average beam pattern.

4. RESHOW is a program which displays any of the maps produced by REDCOR or SKYMAP on the color TV, graphics terminal, or hardcopy device.

b) General Considerations

The TPT is different from most other synthesis-type radio telescopes in that all the Fourier components from a minimum spacing of about one wavelength to the maximum aperture of the system are available simultaneously. Also, the telescope operates in a frequency range where terrestrial interference is very common. It appeared to be necessary to develop procedures to reject low level interference after formation of the maps, as well as to reject obvious interference in the visibility-plane data. Therefore, rather than averaging the visibility-plane data for hours, then gridding them and transforming them, we transform the data frequently and average the selected maps. Since maps are formed frequently, this processing scheme is also more appropriate for observation of rapidly varying solar emission regions.

The length of time over which we can integrate the visibility-plane data before Fourier transformation is limited to ~ 5 minutes; longer integrations would begin to smear the visibility data because of the rotation and foreshortening of the arrays caused by Earth rotation. The T-shaped antenna provides data automatically in a 32×32 grid; we do not project them onto the $(u-v)$ -plane or regrid them before transformation. In practice, a transformation is performed and a new integration is begun whenever the phase gradients across the banks of elements are updated to follow the source under observation. Maps are generally produced at intervals of 1 s to 5 minutes. Use of longer intervals facilitates the processing speed but requires that more data be discarded when interference occurs.

The fringe stopping in REDCOR requires ~ 1 s for each data record of 512 complex correlations; the Fourier transform requires 11 s. Provided that data records are written only at 2 to 10 s intervals and that 1 minute or more of data are integrated before transformation, data processing can be performed more quickly than observing. It will be necessary to employ an array processor to speed up the data processing by orders of magnitude if solar maps are to be produced at 10 to 100 ms intervals.

The TPT is a very thin-armed array with a filling factor that varies from 0.25% at $\lambda = 10$ m to 0.1% at $\lambda = 3$ m. Because of this low filling factor, the system is

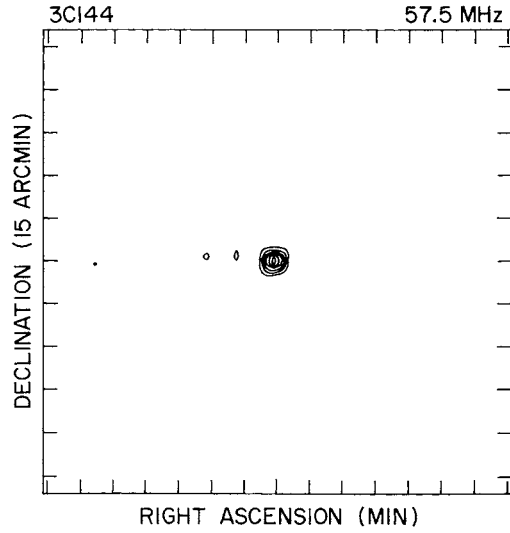


FIG. 9a

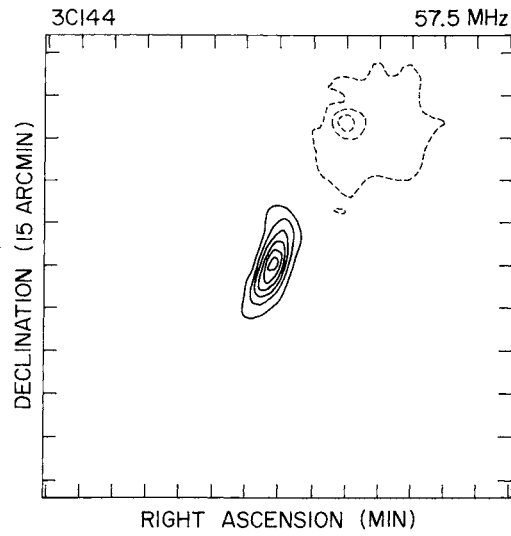


FIG. 9b

FIG. 9.—Maps of the apparent brightness distribution of Tau A as the source is occulted by the solar corona. Contours are linear in brightness. (a) Tau A on 1981 June 30. Angular separation between the Sun and the source was $15^{\circ}1$. This map shows the beam shape with no apparent scattering. (b) Tau A on 1981 June 17; separation was $3^{\circ}13$. The Sun is out of the field to the left; its replicated “ghost” image is above and to the right of Tau A.

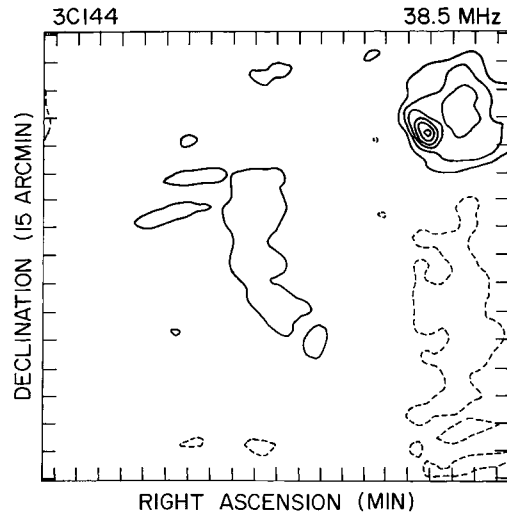


FIG. 9c

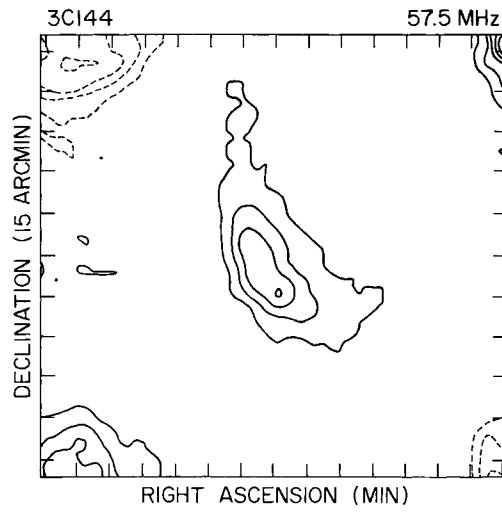


FIG. 9d

FIG. 9. (*Continued*)—(c) Same as (b) except at a lower frequency. The Sun is to the upper right, Tau A is heavily scattered. (d) Tau A on 1981 June 12; separation was $2^{\circ}42'$. Part of the Sun is in the upper right corner; the remaining parts of the solar image are replicated into the other three corners of the map.

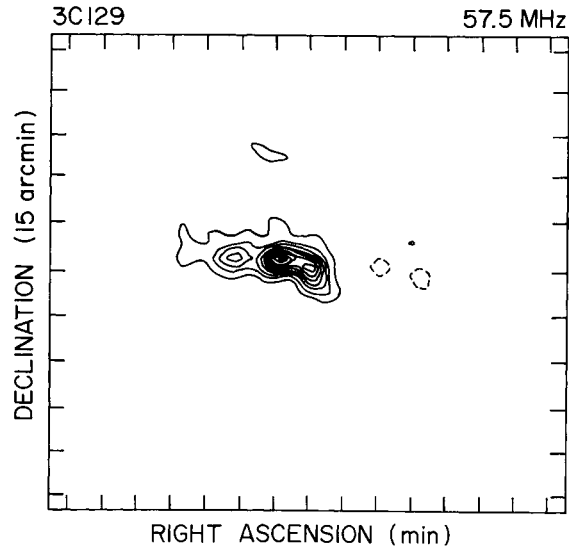


FIG. 10a

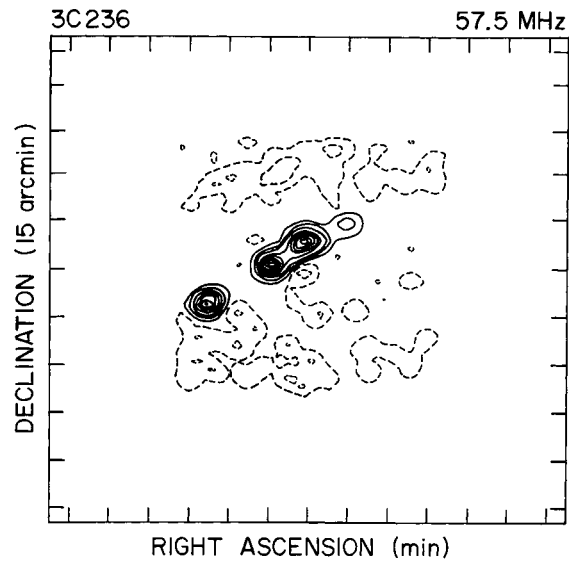


FIG. 10b

FIG. 10.—Maps of several radio sources. The contours are linear in brightness. (a) The radio sources 3C129 and 3C129.1 as observed at 57.5 MHz. The coordinates of the map center are $04^{\text{h}}45^{\text{m}}, 44^{\circ}56'$, (1950). 3C129.1 is observed at the left, almost resolved from the head-tail galaxy, 3C129, which is seen on the right. (b) A map of 3C236 at 57.5 MHz. The map center is at $10^{\text{h}}03^{\text{m}}06^{\text{s}}, 35^{\circ}08'40''$, (1950). The central galaxy and two outer lobes are easily visible in this map, as well as a possible further extension to the NW. The peak component in the map is at 12 Jy. This map resulted from an 88 minute observation employing a 0.75 MHz bandwidth. The rms noise level is 660 mJy per beam area.

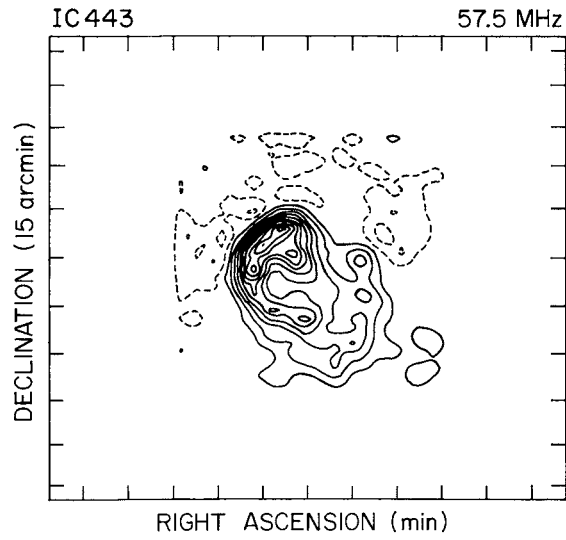


FIG. 10c

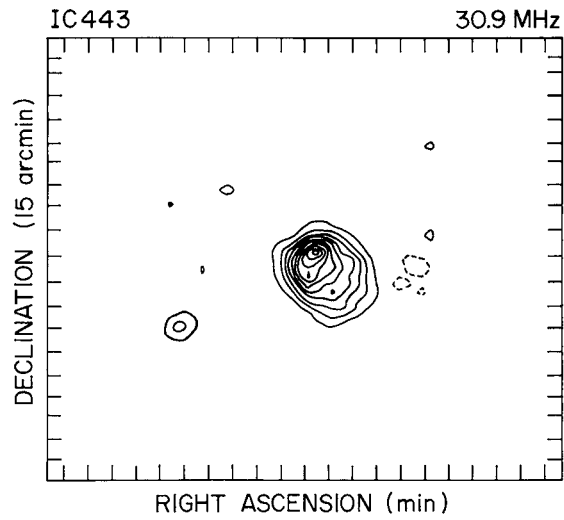


FIG. 10d

FIG. 10. (*Continued*)—(c) The supernova remnant IC 443 at 57.5 MHz. The map center is $06^{\text{h}}14^{\text{m}}36^{\text{s}}, 22^{\circ}43'$, (1950). The 94^{m} observation with a 0.75 MHz bandwidth produced a rms noise level of 1.2 Jy per beam area. (d) Same as (c), but at a frequency of 30.9 MHz. The observation was 97^{m} long and resulted in a rms noise level of 1.60 Jy per beam area.

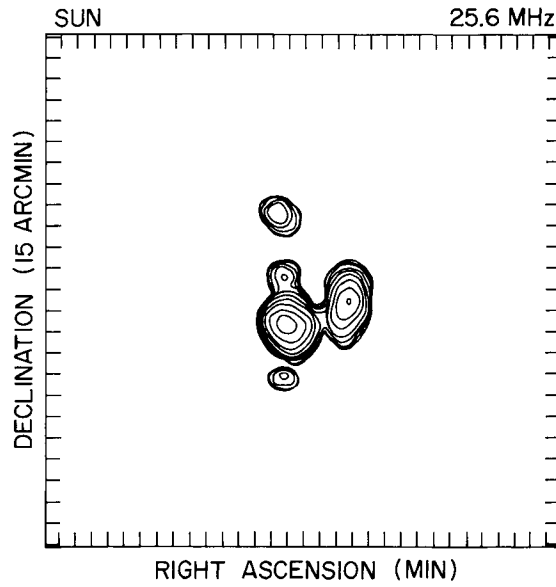


FIG. 11a

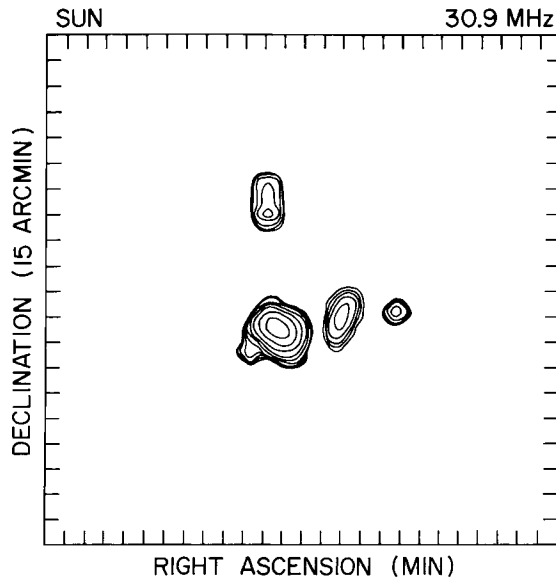


FIG. 11b

FIG. 11.—(a)–(f) Maps of the solar brightness distributions at six frequencies obtained by the TPT on 1981 June 29 are shown. Contours are logarithmic; every contour represents a factor of 2 increase in brightness. Each map covers the full replication field of the system, so the angular scale increases linearly with frequency. The beam size on these maps is thus independent of frequency. Although the apparent angular size of the Sun decreases with frequency, it decreases less rapidly than the scale increases. Thus, the solar image is largest at 110.6 MHz. Below 50 MHz, only nonthermal emission from active regions is seen. Above 50 MHz, the thermal emission from the corona dominates this nonthermal emission.

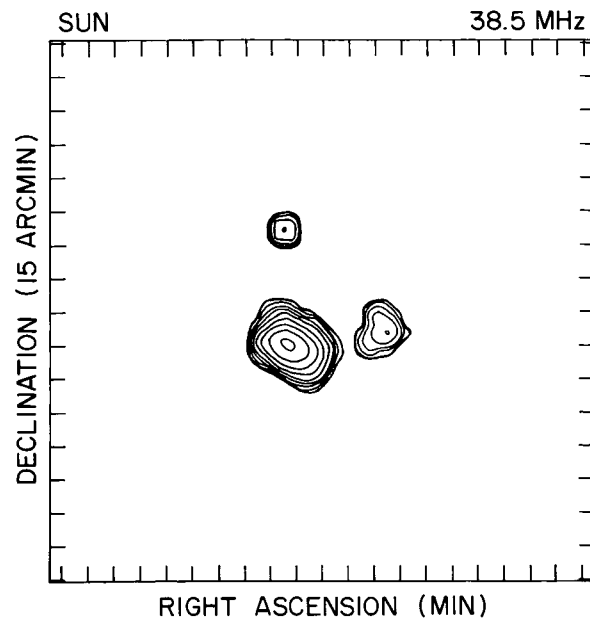


FIG. 11c

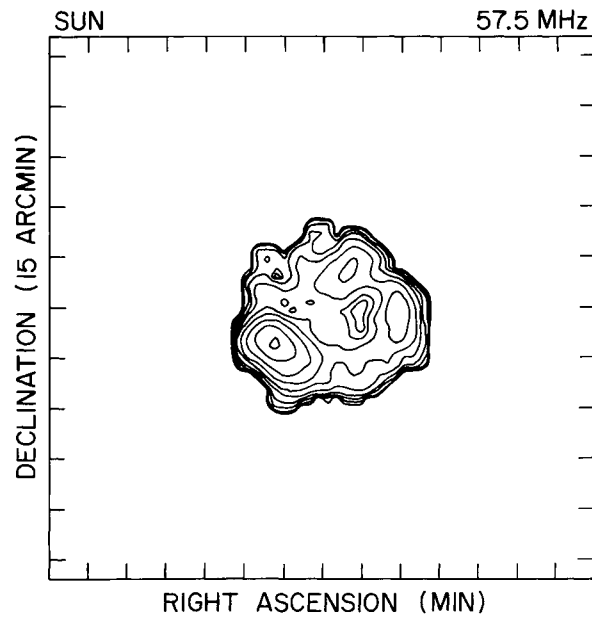


FIG. 11d

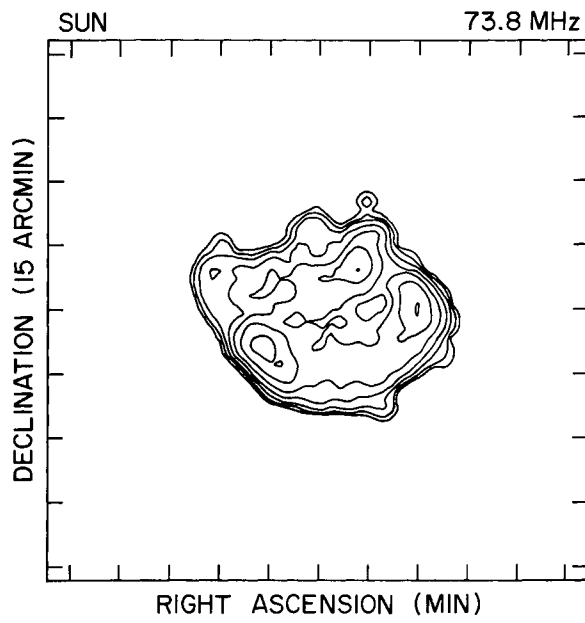


FIG. 11e

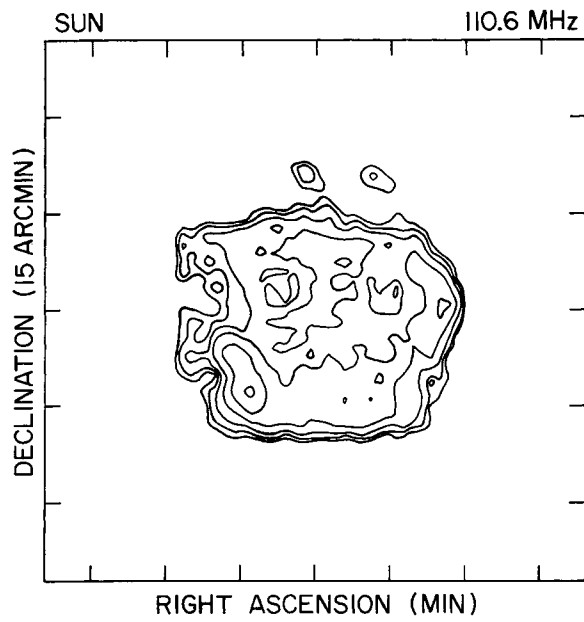


FIG. 11f

basically insensitive to extended, low brightness sources. The system operates well on point sources and on bright extended sources such as the Sun, but for the study of fainter extended sources it is necessary to track the source for 1 hr or more, so that Earth rotation effectively widens the arms. For weak point sources it is also necessary to track the source and integrate in order to reduce the sidelobe responses caused by strong sources in distant sidelobes. After tracking for ~ 1 hr, we achieve a confusion noise level which ranges from 300 to 2000 mJy per beam area. Obviously, this confusion level depends upon position, but it is quite independent of operating frequency, as was predicted by Fisher (1974).

The hardware permits operation with a maximum bandwidth of 3.0 MHz. However, our present experience has indicated that so many observations are spoiled by interference when a 3 MHz bandwidth is employed that it is more practical to use bandwidths of 0.75 or 1.5 MHz. We utilize the frequency bands allocated to radio astronomy to the maximum possible extent since we enjoy some frequency protection in these bands. Often it is necessary to employ bandwidths greater than the protected bands in order to obtain adequate sensitivity. We also search for relatively clear bands and utilize them when we need observations at frequencies between the rather widely spaced radio astronomy bands.

VI. INITIAL RESULTS

Our calibration techniques allow control of the amplitude and phase distribution across the aperture to an accuracy of a few percent. This means that the calculated and observed antenna response patterns agree so well that the differences between them are practically unmeasurable. Also the effective sensitivity of the system is limited primarily by mainlobe and sidelobe confusion. The 1 Jy sensitivity that we have actually achieved is essentially equal to that predicted for the system (Fisher 1974). As mentioned above, some further development is required to make the system applicable for observations of strong, rapidly varying sources such as the active Sun. Our initial results concern stationary or slowly varying objects.

The first concentrated observing effort undertaken with the new system was a series of observations of Tau

A as it was occulted by the outer solar corona in 1981 June. When the angular separation of Tau A and the Sun is less than ~ 40 solar radii, the apparent angular size of Tau A is observed to increase because of coronal scattering. This scattering, caused by magnetically aligned inhomogeneities in the corona, increases rapidly with wavelength and is best measured at long wavelengths. These data provide a direct measurement, in two dimensions, of the spatial spectrum of electron density fluctuations in the solar wind. Tau A is a strong source, and the angular size of the scattering is appropriate for mapping with our system. In total, some 500 maps were made during June, 42 each day. Maps were made at six frequencies each hour during seven hourly sessions. A few examples of the maps that we obtained are shown in Figure 9.

Shown in Figure 10 is a map of the radio source 3C129, a map of 3C236, and two maps of the supernova remnant IC 443. Figure 11 illustrates the brightness distribution of Sun at six frequencies from 25.6 to 110.6 MHz.

VI. SUMMARY

The Clark Lake TPT is a powerful telescope for sidereal and solar radio astronomy at meter-decimeter wavelengths and for ionospheric or magnetospheric science as well. Because it is fully steerable and tunable in frequency, it is a flexible instrument that can be utilized for many different investigations. Our small group at the University of Maryland cannot fully exploit its capabilities; we invite scientists at other institutions to utilize the system as guest observers.

The construction of this system was funded by the National Science Foundation under grant AST-81-08501 and by the National Aeronautics and Space Administration under grant NGR 21-002-199. The land upon which the system is built was donated to the University of Maryland by members of the Burnand family of Borrego Springs, California. Much of the digital design and prototype construction was carried out by Beat von Arx and Mengia Caflisch. The mechanical and electronic construction was performed by Stig and Iva Johansson.

REFERENCES

- Erickson, W. C., and Fisher, J. R. 1974, *Radio Sci.*, **9**, 387.
 Fisher, J. R. 1972, Ph.D. thesis, University of Maryland.
 Högbom, J. A. 1974, *Astr. Ap. Suppl.*, **15**, 417.
 Klinger, R. 1972, M.S. thesis, University of British Columbia.
 von Arx, B., Caflisch, M., and Erickson, W. C. 1978, University of Maryland Rept. AP78-027.

K. ERB: Bodenacherstr. 47, CH-8121 Benglen, Switzerland

W. C. ERICKSON: Astronomy Program, University of Maryland, College Park, MD 20742

M. J. MAHONEY: Clark Lake Radio Observatory, PO Box 128, Borrego Springs, CA 92004